

EMISSION PROPERTIES OF STRUCTURED CARBON FILMS

A.A. EVTUKH, N.I. KLYUI, L.A. KRUSHINSKAYA¹, YU.A. KURAPOV¹,
V.G. LITOVCHENKO, A.N. LUKYANOV, B.O. MOVCHAN¹,
N.A. SEMENENKO

UDC 537.533.2.535.375.54,
535.37,539.231,539.213.2

©2008

V.E. Lashkarev Institute of Semiconductor Physics, Nat. Acad. Sci. of Ukraine
(45, Nauky Ave., Kyiv 03680, Ukraine; e-mail: evtukh@rambler.ru),

¹International Center for Electron Beam Technologies, E.O. Paton Electric Welding
Institute, Nat. Acad. Sci. of Ukraine
(68, Antonovych Str., Kyiv 03150, Ukraine)

Experimental studies of the photoluminescence (PL) and the electron field emission (EFE) of structured carbon films fabricated by electron beam deposition of graphite have been performed. Carbon films were deposited onto the Fe, Fe+Ti, and Si substrates. In the latter case, the Fe catalyst was deposited onto the substrate by electrochemical deposition with the following low-temperature annealing. The key technological parameter for all experiments was the substrate temperature. For additional film characterization, scanning electron microscopy (SEM) and Raman scattering (RS) techniques were used. Intense PL has been observed for films deposited at low temperatures onto Fe and Fe+Ti substrates. The growth of the deposition temperature was accompanied by a decrease of the PL intensity and a shift of the main PL peak toward short wavelengths. The effective electron field emission has been observed from structured carbon films deposited onto a Si substrate with a catalyst. A sharp growth of the emission current and a decrease of the threshold electric field were revealed in the case of structured carbon films deposited at temperatures $T \geq 400$ °C. The following low-temperature annealing in the air environment resulted in a considerable improvement of the EFE parameters. To explain the experimental results obtained, we have proposed a physical model which takes into account the appearance of a band gap in the case of carbon micro- and nanostructures.

1. Introduction

Micro- and nanostructured carbon films – in particular, diamond and diamond-like, carbon nanotubes (CNTs) – are widely applicable owing to their unique properties [1–3]. Owing to a high steepness of their profile, CNTs demonstrate a very efficient field emission. They are conductors and can transmit high currents [4]. It has been shown that a single multiwall CNT can transmit a current with a density up to 10^9 A/cm², which is approximately 1000 times higher than that for copper, the latter being the most widespread conductor in electronic industry [6–8]. CNTs are expected to be one of the most promising materials for future electronics. Therefore, a lot of efforts was spent to develop CNT-

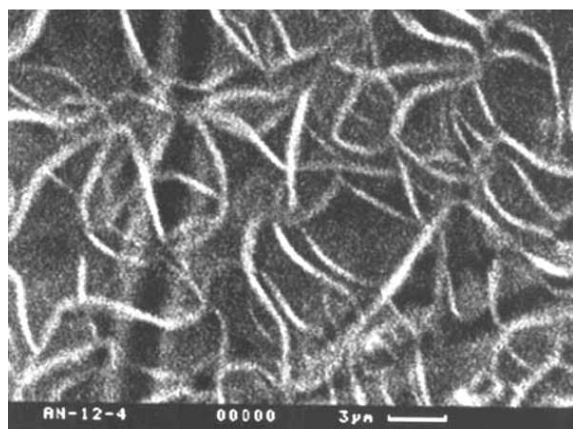
based electronic devices [9–11]. CNTs are also studied in connection with their ability to emit light at the electron field emission [9–11]. CNTs can emit fluorescent light, if they are excited by a laser at a certain wavelength [12]. They can also emit light, if a current is transmitted through a CNT bundle [13].

However, a deterrent to a wide use of structured carbon films, including CNTs, is the low reproducibility of parameters and the low productivity of available technologies – especially in the formation of fullerene compositions, – hence, their high cost. Therefore, there is a necessity for the development of new technologies, for which the listed shortcomings would not be so harmful. One of such technologies is a method proposed by the authors [14–16], where the sputtering of a graphite target in vacuum by a powerful electron beam onto various substrates – both semiconducting and metallic (Fe, Ti, and so on) ones – and at various target temperatures, angles of beam inclination, and other technological parameters is used.

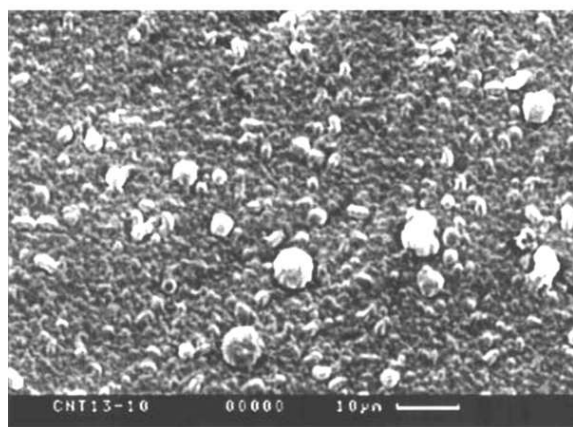
In this work, we report the results of our studies of emission properties of structured carbon films fabricated by the method of electron beam deposition. The features of electron field emission (EFE) and photoluminescence (PL) from micro- and nanostructured carbon films have been studied with respect to the technological conditions of film deposition. For the film characterization, scanning electronic microscopy and Raman spectroscopy (Raman scattering of light) were used as well.

2. Experimental Technique

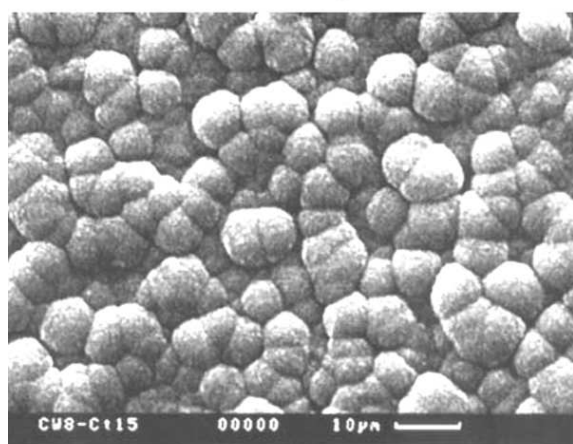
For the fabrication of structured carbon films, the method of electron-beam-induced quick evaporation of graphite in vacuum [14] has been used. Electron beam evaporation of substances in vacuum differs from other methods of vacuum evaporation (thermal and ionic-



a)



b)



c)

Fig. 1. SEM micrograph of the surface of structured carbon films deposited by the electron beam method. The substrate temperature at deposition is $T_s = 110$ (a), 290 (b), and 800 °C (c). Panels a and b correspond to the Fe substrate and panel c to the Fe + Ti one

plasma ones) by its universality, technological flexibility, and profitability [15, 16].

Carbon structures were formed by sputtering graphite with a high degree of purity. Films were deposited onto metal (iron or Fe + Ti; $d = 0.5 \mu\text{m}$) or semiconductor (silicon) substrates at various temperatures in the range 100 – 1100 °C. For the stimulation of carbon nanotube growth, the silicon plates were preliminary covered with a catalyst (iron), making use of the method of electrochemical deposition from a FeSO_4 aqueous solution. Iron deposition was carried out in an electrolytic cell at $U = 40 \text{ V}$ and $I = 250 \text{ mA}$ for 5 min. After the deposition of iron, the silicon substrate was annealed for 45 min at $T = 285 \text{ °C}$ in the air environment. The low-temperature annealing brought about the formation of FeO clusters. After that, the procedure of carbon film deposition was carried out.

The optical properties of the fabricated structures were studied making use of the PL and RS methods. The PL spectra were measured with the nanosecond resolution. For the spectral parameters – peak positions, halfwidths, and amplitudes – to be determined correctly, a decomposition of spectra into those of elementary oscillators (Gaussians) was carried out. The surface morphology of the structures obtained was studied by SEM. In Fig. 1, the micrographs of the surface of structured carbon films deposited at various temperatures are exhibited.

The EFE currents given by specimens were measured in a vacuum system which was pumped out to a pressure of 10^{-5} Pa . The emission current was measured in a structure of the vacuum-diode type. The distance d between the anode and the cathode was maintained constant within the interval from 12.7 to 25 μm . The substrate with the deposited carbon film was used as a cathode, while a flat silicon wafer KES-0.01(100) as an anode. A resistance of 0.56 M Ω was inserted in series into the anode circuit to protect the experimental setup against short circuit and specimen breakdown [17].

All researches were carried out at room temperature.

3. Results and Their Discussion

3.1. Raman scattering

The RS regularities of fabricated films and their dependences on the substrate temperature were studied; the substrate temperature was changed from $T = 100 \text{ °C}$ to high values (more than 500 °C) in the same deposition

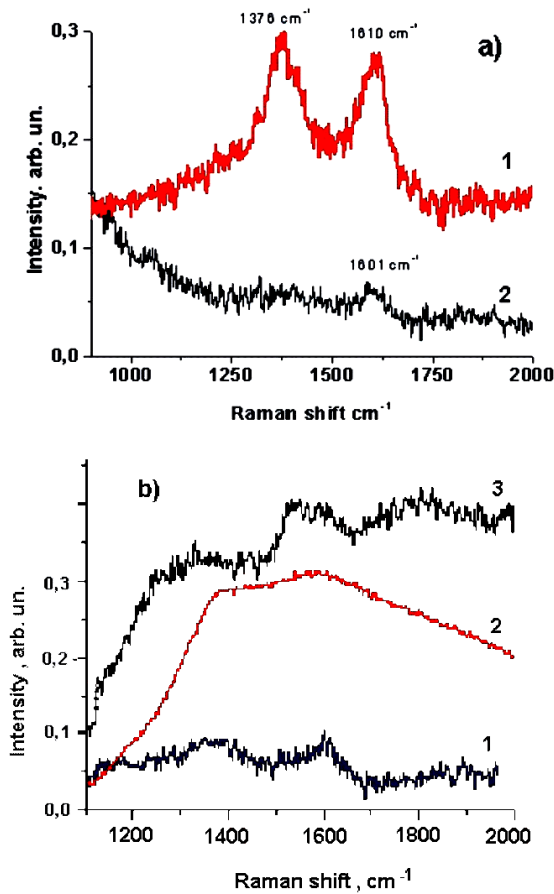


Fig. 2. Raman spectra of light scattered by structured carbon films: (a) 1 – $T = 290$ °C (Fe substrate + $0.5\text{-}\mu\text{m}$ Ti layer), 2 – $T = 290$ °C (Fe substrate); (b) 1 – $T = 500$ °C (Ti substrate), 2 – $T = 150 \div 175$ °C (Ti substrate), 3 – $T = 230 \div 280$ °C (Fe substrate + $0.5\ \mu\text{m}$ Ti layer)

cycle. In particular, the formation of micro- and nanocrystalline structures, which was registered by RS spectra (Fig. 2), turned out more pronounced at low substrate temperatures $T_s \approx 200 \div 300$ °C, whereas, at higher temperatures, $T_s \geq 500$ °C, the spectra became nonstructured, which is typical of the amorphous state of carbon. The structured sections of the spectrum enable one to estimate the dimension and the type of nanocrystallites with the sp^2 chemical bond, as well as to make a conclusion about the availability of defects with a certain configuration (broken bonds or their joining, aggregation or splitting of graphite-like nanoclusters, and so on). Band G is associated with symmetric longitudinal vibrations of C–C bonds (sp^2 -hybridization) in six-atom C_6 -rings at Γ -point of the Brillouin zone in a crystal of the graphite modification with $E = 1581\text{ cm}^{-1}$; the shift to higher frequencies

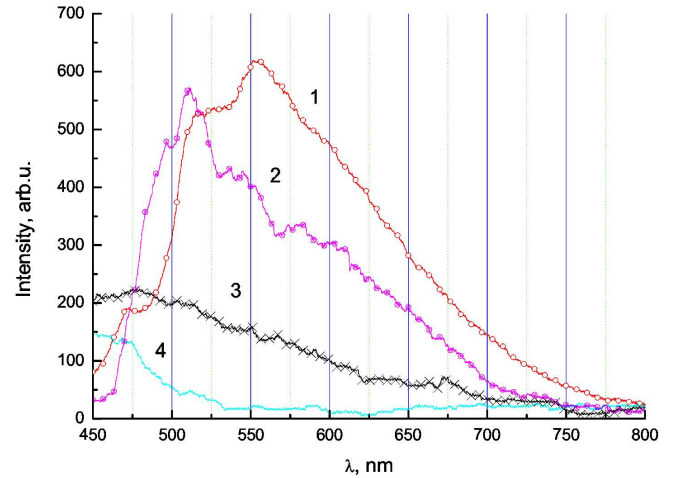


Fig. 3. PL spectra of structured carbon films: 1 – $T = 110$ °C (Fe substrate), 2 – $T = 100$ °C (Fe substrate + $0.5\text{-}\mu\text{m}$ Ti layer), 3 – $T = 290$ °C (Fe substrate + $0.5\text{-}\mu\text{m}$ Ti layer), 4 – $T = 800$ °C (Ti substrate)

($1590 \div 1610\text{ cm}^{-1}$) is caused by a reduction of the crystallite dimensions down to 25 nm, which is followed by the appearance of the line at 1620 cm^{-1} stemming from the violation of selection rules at $q \neq d$ in the vicinity of Γ -point [3]. For nanocrystals, a prohibition of transitions with participation of phonons in the vicinity of the $K = 0$ point of the Brillouin zone is cancelled, which gives rise to the emergence of a defective D -band at 1355 cm^{-1} . This band is associated with vibrations that satisfy the condition $q \approx 2k$, where k is the wave vector of electrons participating in vibration transitions. That is, the quasiselection rule in six-atom aromatic rings is fulfilled. Hence, the availability of D -band is an indicator of graphite-like nanoclusters. A sharp peak at 1338 cm^{-1} produced by the diamond crystal phase was not observed in our experiments. At the same time, a peak in the vicinity of 1376 cm^{-1} was observed, although it was substantially smeared in most cases (Fig. 2,a). The most arranged films turned out those which had been deposited at $T \approx 290$ °C.

3.2. Photoluminescence

In Fig. 3, some examples of PL spectra obtained for specimens fabricated on the Fe substrate (curves 1 and 4) and the Fe substrate with a Ti interlayer (curves 2 and 3) are presented. Curves 1 and 2 correspond to PL of specimens produced at low temperatures of the substrate (110 and 100 °C, respectively), while curves 3 and 4 are the PL spectra of specimens deposited onto

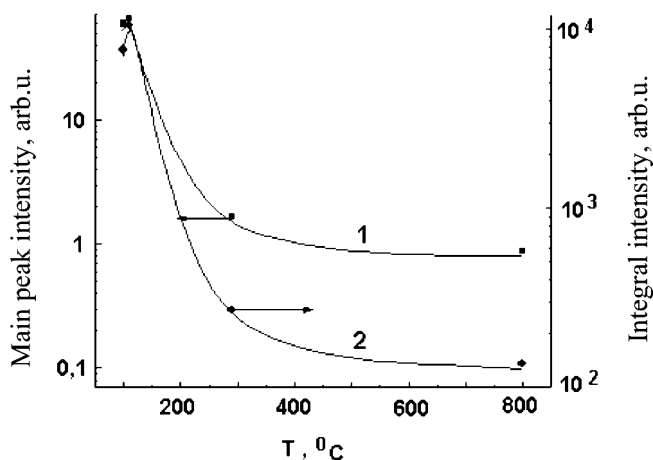


Fig. 4. Dependences of the PL intensity of structured carbon films on the deposition temperature: 1 – the intensity of the main peak, 2 – the integrated intensity

substrates with temperatures of 290 and 800 °C, respectively. As is seen from the figure, the increase of the substrate temperature induces a shift of the main PL peak toward the short-wave range and a simultaneous reduction of the PL intensity, irrespective of the substrate type. The decomposition of the spectrum into Gaussian-like contributions demonstrates that, at low temperatures, the specimens on Fe substrates have two rather wide and intense peaks at wavelengths of 570 and 600 nm, as well as two narrow peaks with low intensities near 530 and 550 nm. The specimens on substrates with a Ti interlayer are characterized by a single, wide enough peak at a wavelength close to 570 nm and two narrow peaks with the same intensities at wavelengths close to 470 and 530 nm.

In Fig. 4, the temperature dependences of the integrated PL intensity (curve 2) and the intensity of the main PL peak (curve 1) are depicted. One can see that the increase of the substrate temperature up to $T \approx 400$ °C leads to a reduction of the PL intensity by 2 to 3 orders of magnitude. The further increase of the deposition temperature weakly affects the PL intensity which becomes rather low.

The PL spectra were analyzed within the framework of the model of coexisting sp^2 (dominating) and sp^3 (defective) bond hybridization [1–3]. The shift of the main PL peak toward the short-wave range of the spectrum, which accompanies the growth of T_s (Fig. 3), testifies to a higher and higher probability of the formation of sp^3 configurations for local bonds. Some evidence for such a scenario is the emergence of a weakly pronounced peak at a frequency of 1332 cm^{-1} in the

RS spectra of some specimens (Fig. 2). The formation of micro- and nanocrystals from graphite gives rise to a strong deformation of sp^2 bonds. In particular, the bend of a sheet composed of sp^2 bonds into a nanotube brings about a change of the sp^2 -bond configuration and their approach to the bonds of the sp^3 type [18]. A transformation from the sp^2 hybridization to the sp^3 one is accompanied by a modification in the corresponding electron density of states by means of a reduction of the overlapping between π -bands near the Fermi level of the material. Since semimetallic properties of crystalline graphite are governed by the overlapping between π -bands, the deformation of an atomic layer results in a reduction of the overlapping and stimulates carbon to undergo a phase transition belonging to the semimetal–semiconductor type [19, 20]. The possibility of such a transition for microcrystalline carbon has been shown theoretically in work [20], where the strong-coupling approximation was used.

SEM micrographs of the surface of films under investigation evidence for the availability of micro- and nano-sized asperities, which confirms the possibility of the semimetal–semiconductor transition. In the case of carbon nanotubes, sp^3 -like atomic configurations will be arranged along the lateral surface of a nanotube.

It should be noted that a rise of the substrate temperature not only reduces the PL intensity, but also invokes drastic structural modifications. According to scanning microscopy data, structured carbon films on iron substrates are characterized at low temperatures by a threadlike structure with a thread diameter of $0.3 \div 0.6\ \mu\text{m}$; on titan substrates, there emerge the clusters with a more uniform size distribution ($10\ \mu\text{m}$ and less). As the temperature grows, the threadlike structure transforms into a clusterlike one, while – in the case of titan substrates – the dimensions of clusters diminish, but their spread increases. In spite of different structures of carbon films on iron and titan substrates, those obtained at the substrate temperature $T \approx 100$ °C demonstrate intense PL.

3.3. Electron field emission

The structured carbon films deposited onto silicon substrates by applying the method of electron beam deposition revealed good EFE parameters in a wide range of deposition temperatures (from about 100 to 1140 °C). In Fig. 5,a, the emission current-voltage characteristics (CVCs) of the structured carbon films deposited onto silicon substrates with a catalyst (Fe) are depicted; in Fig. 5,b, the same dependences are

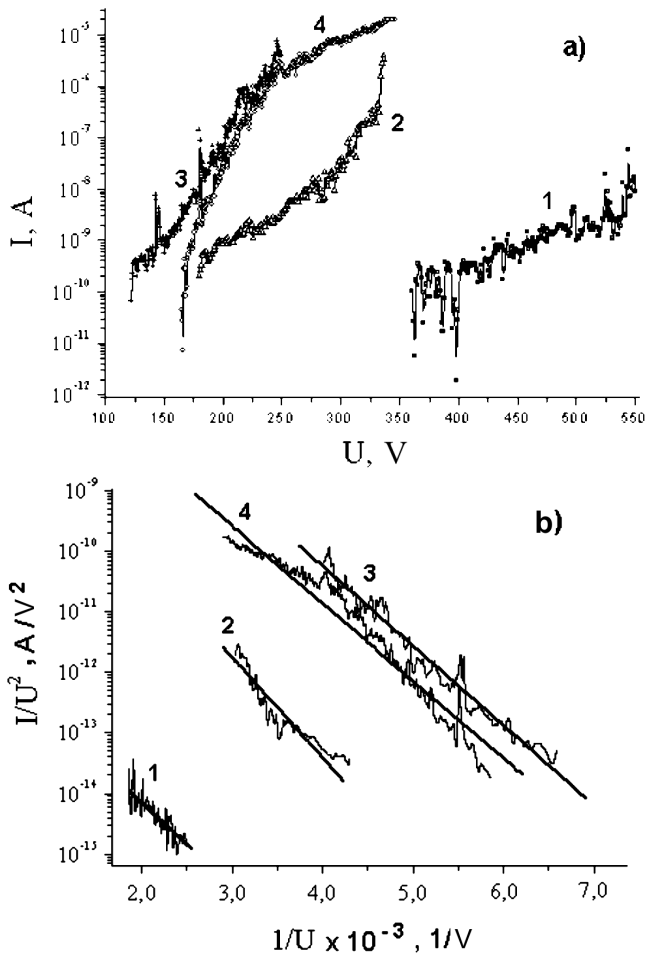


Fig. 5. (a) Emission CVCs of structured carbon films deposited by the electron beam method onto silicon substrates with a catalyst (Fe) and (b) the same dependences in the Fowler–Nordheim coordinates for various deposition temperatures $T = 270$ (1), 380 (2), 537 (3), and 1032 °C (4)

plotted in the Fowler–Nordheim coordinates. The CVCs are typical of the EFE in vacuum; as the temperature of the carbon material deposition increases, the shift of the curves obtained toward the low-voltage region is observed. From Fig. 5, *b*, it is evident that the films deposited at low temperatures are characterized by a low emission current. This fact may be possibly associated with low adhesion of carbon material to the substrate. If it is so, the field erosion of a carbon film on the cathode is probable at high electric fields. At higher deposition temperatures (> 400 °C), the field emission current drastically increases; however, the plots have the same slope in the Fowler–Nordheim coordinates (Fig. 5, *b*), which testifies to the invariance of both the surface microrelief geometry and the work function of a film

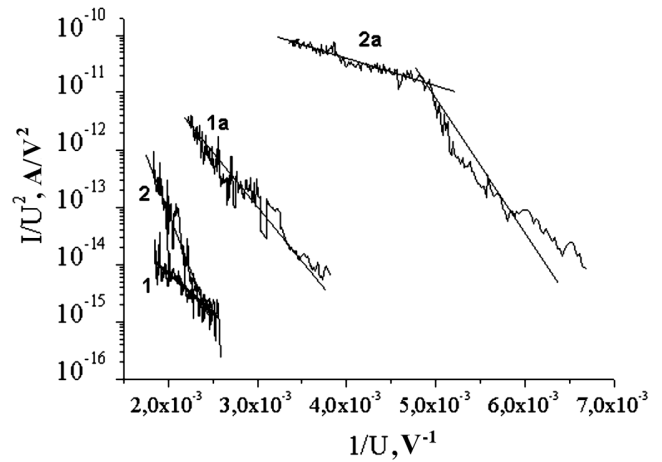


Fig. 6. Emission dependences of structured carbon films deposited by the electron beam method onto silicon substrates with a catalyst (Fe) before (curves 1 and 2) and after (curves 1a and 2a) thermal annealing in the air environment: 1 – $T = 270$ °C, 2 – $T = 677$ °C, 1a and 2a – after additional annealing $T = 350$ °C

material; nevertheless, the effective emission surface, i.e. the total number of microcathodes, increases.

In order to enhance EFE from structured carbon films, the researches of the influence of the additional thermal annealing of specimens on the EFE efficiency were fulfilled. In Fig. 6, the emission dependences of the structured carbon films measured before and after thermal annealing in air at a temperature of 350 °C and for 60 min are plotted in the Fowler–Nordheim coordinates. From this figure, it is evident that thermal annealing does not result in a substantial change of the slope of emission dependences. The invariance of this slope – if to compare the dependences before and after annealing – testifies that the surface morphology (the surface asperities, from which emission mainly occurs), as well as the nature of emitting substance, remained practically invariant. The improvement of EFE parameters (a shift to the low-voltage range, an increase of emission currents) after annealing takes place, in our opinion, owing to the increase of the emitting surface area α (the number of emitting centers) (see Table). The thermal treatment of specimens, due to the interaction of carbon with oxygen and the moisture of air, removes amorphous modifications of carbon from the film. At the same time, the phase of micro- (nano-) crystalline carbon is more stable to the thermal treatment than the amorphous phase; therefore, the former remains in the cathode film.

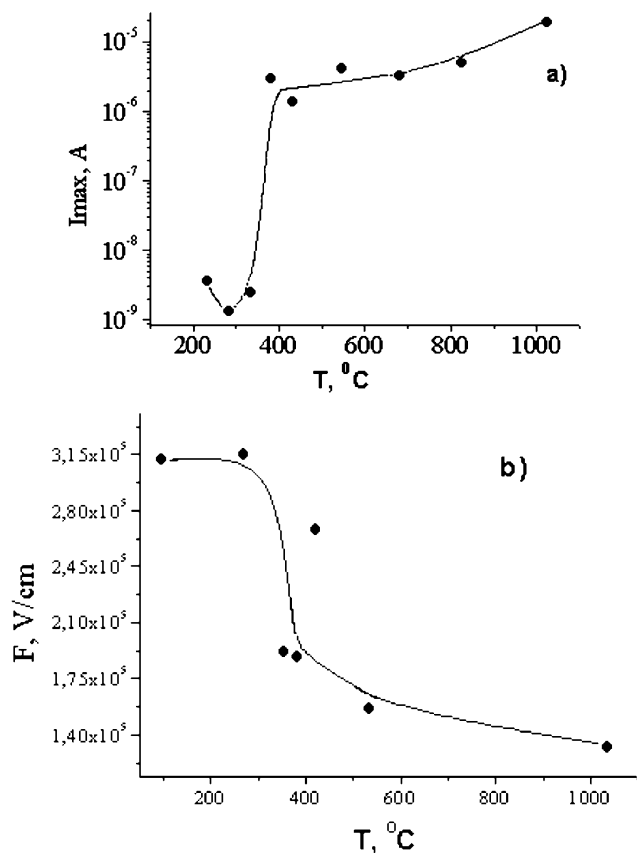


Fig. 7. Dependences of the maximal emission current (a) and the threshold electric field (b) at EFE from structured carbon films deposited by the electron beam method onto silicon substrates with a catalyst (Fe) on the substrate temperature

The dependences of the maximal (pre-breakdown) emission current and the threshold electric field on the substrate temperature (at deposition) for the EFE from structured carbon films are shown in Fig. 7. A substantial change of the EFE current from structured carbon films deposited at $T \geq 400$ °C is evident. The specimens that have been obtained at higher deposition temperatures are characterized by higher levels of the emission current; in particular, the current increases

by three orders of magnitude and reaches the values of $10^{-6} \div 10^{-5}$ A (the maximal current density was $1.5 \div 2$ mA/cm²). As is seen from Fig. 7, b, the threshold macroscopic electric field of the emission from films deposited at $T \geq 400$ °C falls within the range of $(1.4 \div 1.8) \times 10^5$ V/cm. It only slightly exceeds the threshold electric field of the emission from carbon nanotubes which is equal to $(1 \div 9) \times 10^4$ V/cm [21].

The key EFE parameters of the structured carbon films obtained in this work making use of the electron beam method are listed in Table. While calculating the EFE parameters, the emission CVCs were simulated for every specimen. In calculations, the values of the work function were selected fixed and typical of the graphite carbon phase; namely, the selected value of the work function was 4.7 eV, which is characteristic of graphite [22]. As is seen from Table, the increase of the deposition temperature improves the EFE efficiency of structured carbon films, reduces the threshold electric fields, and enlarges both the emission current and the effective emission area α .

The values $\beta^* = 220 \div 290$ obtained for the electric field gain factor from the slope of emission curves in the Fowler–Nordheim coordinates at a given work function (4.7 eV) turned out higher than the relevant values calculated from the surface relief geometry, $\beta^* \approx h/r$, where h is the height of a spike, and r is the curvature radius of its tip. A better agreement can be reached, if one starts from the model which takes into account the coexistence of carbon phases with the bonds of the sp^2 - (graphite-like) and sp^3 - (tetrahedral) configurations. The corresponding model of coexisting sp^2 - and sp^3 -configurations in strongly deformed C–C carbon structures is shown in Fig. 8, a for two variants of fabrication technology: with the domination of sp^2 graphite-like nanoclusters or with dominating sp^3 diamond-like nanoclusters.

The emergence of the energy gap in nanotubes has to bring about a reduction of the work function at large fields (Fig. 6, curve 2a), in accordance with the model depicted in Fig. 8 [23].

EFE parameters for structured carbon films deposited by the electron beam method onto silicon substrates with a catalyst

N of specimen	Deposition mode		EFE parameters					
	T_d	t_d , c	U_{th} , B	Φ^* , eV	β^*	I_{min} , A	I_{max} , A	α , cm ²
D1	270	45	400	4.7	270	2.5×10^{-10}	1.1×10^{-9}	3×10^{-18}
4C	380	20	242	4.7	223	2.1×10^{-9}	3.3×10^{-6}	1.84×10^{-13}
D4	537	45	200	4.7	281	5.8×10^{-10}	4.2×10^{-6}	7.4×10^{-12}
D5	677	45	340	4.7	220	7.4×10^{-7}	3×10^{-6}	8.84×10^{-15}
5F	1032	20	170	4.7	290	1.4×10^{-10}	2×10^{-5}	1.2×10^{-12}

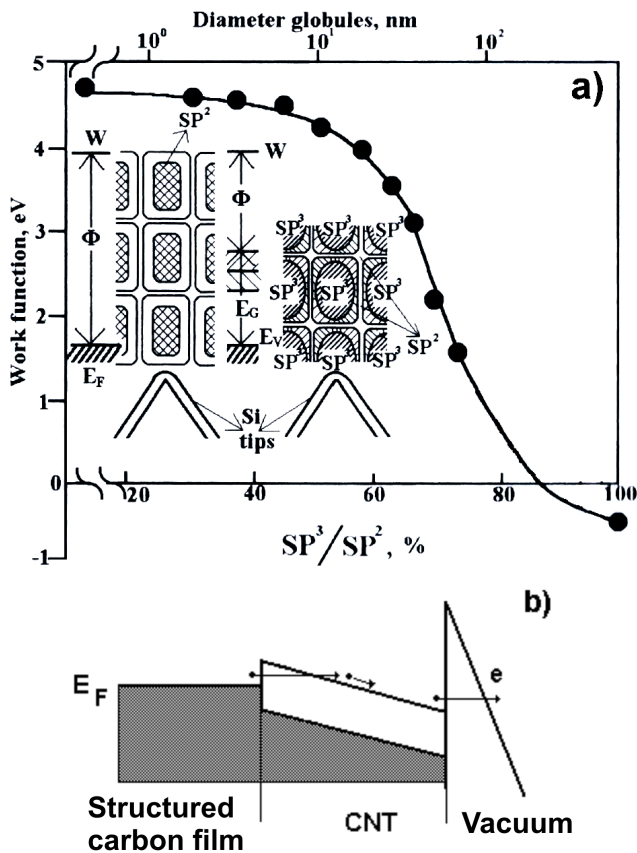


Fig. 8. (a) Dependence of the work function for diamond-like carbon films on the ratio sp^3/sp^2 . The inset illustrates the film models with the formation of sp^2 graphite-like nanoclusters and sp^3 diamond-like clusters. (b) Energy band diagram of the structure and the scheme of current transmission at the electron field emission from carbon nanotubes

4. Conclusions

The emission properties of structured carbon films deposited making use of the electron beam sputtering of graphite have been studied. The critical parameters, which were varied at the deposition, were the substrate temperature $T = 100 \div 1100$ °C and the substrate material (Fe, Fe + Ti, Si).

An intense PL from the structured carbon films deposited at low temperatures onto Fe and Fe + Ti substrates has been revealed. The growth of the deposition temperature was accompanied by a reduction of the PL intensity and a shift of the main PL peak toward the short-wave range, up to the complete disappearance of PL. On the contrary, the current of the electron field emission from structured carbon films deposited at elevated temperatures ($T \geq 400$ °C) on the

Si substrate covered with a catalyst was rather high. The threshold electric fields were $(1.4 \div 1.8) \times 10^5$ V/cm, and the emission current densities were 1.5–2 mA/cm². In addition, the low-temperature thermal annealing in air substantially improved the EFE parameters and did not influence PL essentially.

To explain the obtained emission data, we have proposed a physical model which makes allowance for the emergence of the energy gap in the case of carbon micro- and nanostructures.

Hence, in order to obtain carbon films with good luminescence, one should choose low-temperature regimes of film deposition; whereas, if a good emission is desirable, the deposition should be carried out at elevated temperatures. We explain these features in the framework of the model presented in Fig. 8; namely, as the deposition temperature grows, the width of the energy gap increases (owing to the growth of the sp^3 -component, Fig. 3,a, the PL peak shifts toward the short-wave range of the spectrum), due to the increase of distortions of C=C hexagonal bonds and, therefore, to the increase of the number of centers of radiationless recombination; the latter process, on the contrary, induces a reduction of the photoemission ability of the films.

Thus, for the fabrication of light-emitting structures (luminescent sources of light), low-temperature carbon structures should be used; for the electric excitation of the luminescence of films, on the contrary, the carbon films prepared at high temperatures and possessing a high electron-emission ability are more effective.

1. V. Litovchenko and A. Evtukh, in *Handbook of Semiconductor Nanostructures and Nanodevices, Vol. 3: Spintronics and Nanoelectronics*, edited by A.A. Balandin and K.L. Wang (American Scientific Publishers, Los Angeles, 2006), p. 153.
2. V.G. Litovchenko, *Ukr. J. Phys.* **44**, 1064 (1999).
3. E.A. Smorgonskaya and V.I. Ivanov-Omskii, *Fiz. Tekh. Poluprovodn.* **39**, 970 (2005).
4. W. Zhu, C. Bower, O. Zhou, G. Kochanski, and S. Jin, *Appl. Phys. Lett.* **75**, 873 (1999).
5. B.Q. Wei, R. Vajtai, and P.M. Ajayan, *Appl. Phys. Lett.* **79**, 1172 (2001).
6. C. Dekker, *Phys. Today* **52**, 22 (1999).
7. Q.H. Wang, T.D. Corrigan, and R.P.H. Chang, *Appl. Phys. Lett.* **70**, 3308 (1997).
8. P.G. Collins and A. Zettl, *Phys. Rev. B* **55**, 9391 (1997).
9. J.M. Bonard, T. Stochls, F. Maier, W.A. De Heer, A. Chatelain, J.P. Salvetat, and L. Forro, *Phys. Rev. Lett.* **81**, 1441 (1998).
10. M. Sveningsson, M. Jonsson, O.A. Nerushev, F. Fohmund, and F.E.B. Campell, *Appl. Phys. Lett.* **81**, 1095 (2002).

11. J. Wei, H. Zhu, and D. Wu, *Appl. Phys. Lett.* **84**, 4869 (2004).
12. S.M. Bachilo, M.S. Strono, C. Kittrell, R.H. Hauge, R.E. Smalley, and R.B. Weisman, *Science* **298**, 2361 (2002).
13. P. Li, K.L. Jiang, M. Liu, Q.Q. Li, and S.S. Fan, J.L. Sun, *Appl. Phys. Lett.* **82**, 1763 (2003).
14. B.A. Movchan *et al.*, US Patent 5296274A from 22.03.1994.
15. B.A. Movchan, *Nanosyst. Nanomater. Nanotekhnol.* **2**, 1103 (2004).
16. B.A. Movchan, *Surf. Eng.* **22**, 35 (2006).
17. A.A. Evtukh, H. Hartnagel, V.G. Litovchenko *et al.*, *Semicond. Sci. Technol.* **19**, 923 (2004).
18. H. Hiura, T.W. Ebessen, J. Fujita, K. Tanigaki, and T. Takada, *Nature* **367**, 148 (1994).
19. R. Grigorovici, A. Devenji, A. Greoghiu, and A. Belu, *J. Non-Cryst. Solids* **8–10**, 793 (1972).
20. V.I. Gavrilenko, N.I. Klyui, V.G. Litovchenko, and V.E. Strelnitskii, *Phys. Status Solidi B* **145**, 209 (1988).
21. S.-C. Chean, L.-Y. Shih, Y.-C. Chang, G.-C. Tu, and I-N. Lin, *J. Vac. Sci. Technol. B* **19**, 1026 (2001).
22. V.S. Fomenko, *Emission Properties of Elements and Chemical Compounds* (Naukova Dumka, Kyiv, 1980) (in Russian).
23. V.G. Litovchenko, A.A. Evtukh, and M.I. Fedorchenko, *Mater. Sci. Eng. A* **353**, 47 (2003).

Received 20.07.07.

Translated from Ukrainian by O.I. Voitenko

ЕМІСІЙНІ ВЛАСТИВОСТІ ВУГЛЕЦЕВИХ СТРУКТУРОВАНИХ ПЛІВОК

А.А. Євтух, М.І. Кльої, Л.А. Крушинська, Ю.А. Курапов,
В.Г. Литовченко, А.М. Лук'янов, Б.О. Мовчан,
М.О. Семененко

Резюме

Проведено експериментальні дослідження фотолюмінесценції (ФЛ) та електронної польової емісії (ЕПЕ) вуглецевих структурованих плівок, отриманих електронно-променевим осадженням графіту. Вуглецеві плівки осаджувались на підкладки з Fe, Fe+Ti та Si. На кремнієві підкладки попередньо наносили каталізатор (Fe) методом електрохімічного осадження та після цього проводили низькотемпературний відпал. Основним технологічним параметром, що змінювався при осадженні вуглецевих плівок, була температура підкладки. Для додаткового дослідження плівок використовували скануючу електронну мікроскопію та комбінаційне розсіяння світла (КРС). Виявлено інтенсивну ФЛ плівок, осаджених при низьких температурах на Fe- та Fe+Ti-підкладки. З ростом температури осадження відбувалось зменшення інтенсивності ФЛ та зсув основного піка в короткохвильовий бік. Спостерігалась ефективна ЕПЕ вуглецевих структурованих плівок, осаджених на кремнієву підкладку з каталізатором. Виявлено різке зростання емісійного струму та зменшення порогового електричного поля у випадку вуглецевих структурованих плівок, отриманих при $T \geq 400$ °C. Подальший низькотемпературний термічний відпал на повітрі приводить до суттєвого поліпшення параметрів ЕПЕ. Для пояснення отриманих експериментальних результатів з ФЛ та ЕПЕ запропоновано фізичну модель, яка припускає появу забороненої зони у вуглецевих мікро- та наноструктурах.